Mycopathologia (2016) 181:631–642
DOI 10.1007/s11046-016-0029-0

Impairment of Immune Response against Dematiaceous Fungi in *Card9* Knockout Mice

Weiwei Wu · Ruijun Zhang · Xiaowen Wang · Yinggai Song · Zhengyang Liu · Wenling Han · Ruoyu Li

Received: 24 March 2016 / Accepted: 12 June 2016 / Published online: 15 July 2016

Abstract Dematiaceous fungi are a large group of pathogens that can cause a wide range of diseases in both immunocompetent and immunocompromised hosts. Based on our previous finding of caspase recruitment domain-containing protein 9 (*CARD9*) mutations in patients with subcutaneous phaeohyphomycosis caused by *Phialophora verrucosa* (*P. verrucosa*), we further investigated the exact role of CARD9 in the pathogenesis of phaeohyphomycosis using *Card9* knockout (*Card9* KO) mice. We showed that *Card9* KO mice are profoundly susceptible to *P. verrucosa* infection compared with wild-type mice, reflected by significantly more severe footpad swelling, higher fungal burden, lower survival, and systemic dissemination. The inability of *Card9* KO mice to control *P. verrucosa* infection was associated with lack of Th17 differentiation and reduction of tumor necrosis factor (TNF)-α, interleukin (IL)-1β, IL-6, and IL-17A levels in footpad homogenates. In vitro experiments showed a defect of fungal conidia killing and pro-inflammatory cytokine production in *Card9* KO bone marrow-derived macrophages and dendritic cells. Furthermore, ex vivo coculture and in vitro T cell differentiation assay demonstrated that Card9 signaling pathway acts indispensably on differentiation of Th17 cells. In conclusion, our findings suggest that CARD9 mediate the innate immune and Th17-mediated adaptive immune responses against dematiaceous fungal infections at the early stage of infection.

Keywords *Phialophora verrucosa* · CARD9 · Murine model · Macrophages · Dendritic cells · Th17

Weiwei Wu and Ruijun Zhang have contributed equally to this work.

Electronic supplementary material The online version of this article (doi:10.1007/s11046-016-0029-0) contains supplementary material, which is available to authorized users.

W. Wu · R. Zhang · X. Wang · Y. Song · R. Li
Department of Dermatology, Peking University First Hospital, Beijing, China

W. Wu · R. Zhang · X. Wang · Y. Song · R. Li
Research Center for Medical Mycology, Peking University, Beijing, China

W. Wu · R. Zhang · X. Wang · Y. Song · R. Li (✉)
Beijing Key Laboratory of Molecular Diagnosis on Dermatoses, Beijing, China
e-mail: mycolab@126.com

Z. Liu · W. Han
Department of Immunology, School of Basic Medical Sciences, Peking University Health Science Center, Beijing, China

Z. Liu · W. Han
Peking University Center for Human Disease Genomics, Beijing, China

Z. Liu · W. Han
Key Laboratory of Medical Immunology, Ministry of Health, Beijing, China

Introduction

Dematiaceous fungi, the so-called black yeasts, comprise a large group of pathogens characterized by the presence of melanin in their cell walls. Dematiaceous fungi are often found in the soil and are distributed extensively worldwide. These melanized fungi are responsible for a wide range of chronic cutaneous, subcutaneous, systemic, or disseminated infections in both immunocompetent and immunocompromised individuals, including phaeohyphomycosis, chromoblastomycosis, and mycetoma [1–3]. Dematiaceous fungi have increasingly received research attention because of the rising incidence of infections related to these life-threatening pathogens and associated difficulties in treatment, particularly in immunocompromised patients. However, the basic pathogenesis of dematiaceous fungi infections remains poorly understood.

Previous studies have demonstrated that both innate and adaptive immune responses are required for effective containment of fungal infections [4, 5]. Among the innate immune cells, macrophages and neutrophils play important roles in controlling fungal growth through phagocytosis, direct pathogen killing, and secretion of pro-inflammatory factors. Dendritic cells (DCs) are the most powerful antigen-presenting cells (APCs), which trigger adaptive T cell responses against fungal infection. Elimination of fungal spores is considered to principally rely on innate immune cells; however, increasing evidence has emerged to support a role of T-cell-mediated immune responses against fungal infection. Traditionally, responses by interferon-gamma (IFN-γ)-producing Th-1 cells are considered to confer protective immunity against fungi, whereas Th-2 responses mediated by interleukin (IL)-4 lead to increased susceptibility to fungal infections [6]. More recently, a new subset of T helper cells, IL-17-producing Th17 cells, have been identified and were suggested to mediate the immune defense response against extracellular bacteria and fungi [7].

We previously reported four patients with pheohyphomycosis harboring homozygous or compound heterozygous mutations in the caspase recruitment domain-containing protein 9 gene (*CARD9*), which was the first study to link CARD9 with dematiaceous fungal infections. Our data showed that patients lacking CARD9 protein expression showed impaired Th17 cell immune responses to *Phialophora verrucosa* (*P. verrucosa*) [8]. CARD9 is an essential adaptor protein, which is expressed in various tissues, including the spleen, liver, placenta, and lung, with predominant expression in myeloid cells, especially neutrophils, macrophages, and DCs [9]. Following the downstream engagement of several C-type lectin receptors and Syk kinase phosphorylation, CARD9 interacts with B cell lymphoma 10 (BCL10) and mucosa-associated lymphoid tissue lymphoma translocation gene 1 (MALT1), and then triggers nuclear factor-kappa B (NF-κB) activation to initiate the downstream adaptive immune response [10]. Lack of CARD9 has recently been reported to result in severe susceptibility to different fungal infections such as chronic mucocutaneous candidiasis, *Candida* meningoencephalitis, deep dermatophytosis, phaeohyphomycosis, *Exophiala* disease, and *Corynespora cassiicola* infection [8, 11–15]. Therefore, the Syk-CARD9 pathway appears to play an essential role in antifungal immunity because of the convergent role of innate and adaptive antifungal immune responses. However, the role of CARD9 in the pathogenesis of dematiaceous fungal infections is yet to be elucidated.

In recent years, the fungal species *P. verrucosa* has emerged as a major pathogenic dematiaceous fungus in China [16, 17]. In this study, we used *P. verrucosa* as a representative strain of dematiaceous fungi and established murine and cellular models of infection to further decipher the role of CARD9 in the development of protective immunity during dematiaceous fungal infection.

Materials and Methods

Experimental Animals

Animal experiments were performed on C57BL/6 wild-type (WT) mice (Vital River Laboratories, Beijing, China) and *Card9* knockout (KO) mice (C57BL/6 background), which were generously provided by Dr. Xin Lin (MD Anderson Cancer Center, Houston, TX, USA). All experiments included age- and sex-matched controls with the C57BL/6 background. All mice were maintained in specific pathogen-free facilities at the Institute of Clinical Pharmacology of Peking University according to institutional guidelines.

Conidia Preparation and Labeling

The *P. verrucosa* strain was obtained from a clinical CARD9-deficient patient with phaeohyphomycosis. To prepare fungal inocula, *P. verrucosa* isolates were cultured on oatmeal agar (Becton–Dickinson Biosciences, San Diego, CA, USA) for 14–21 days at 28 °C. Conidia were heat-killed at 100 °C for 30 min. Fluorescein isothiocyanate (FITC)-labeled *P. verrucosa* conidia were prepared with FITC isomer I (Cat No: F7250, Sigma-Aldrich, St. Louis, MO, USA), and the homogeneous distribution of FITC-*P. verrucosa* was confirmed by a flow cytometry assay as previously described [18] (data not shown).

Establishment of a Phaeohyphomycosis Model in *Card9* KO Mice

Groups of WT or *Card9* KO mice were injected subcutaneously with 100 μL of 1×10^8 CFU/mL live *P. verrucosa* conidia into two hind footpads. Survival rates were monitored for 3 months following infection. Disease progression was assessed weekly by measuring footpad swelling using a micrometric caliper. Fungal burdens in the infected footpads were determined by plating serially diluted footpad homogenates on Sabouraud's agar (Becton–Dickinson Biosciences, San Diego, CA, USA). For histological analysis, tissue sections were stained with hematoxylin and eosin (H&E) and Periodic Acid-Schiff (PAS).

Cell Preparation and Culture

Primary cultures of murine bone marrow-derived macrophages (BMDMs) or DCs (BMDCs) were prepared as previously described with minor modifications [19, 20]. In short, BMDMs were differentiated from freshly isolated murine bone marrow cells in complete Dulbecco's modified Eagle's medium (DMEM) containing 30 % conditioned medium from L929 cells expressing macrophage colony-stimulating factor for 5–7 days. Flow cytometry analysis revealed ≥90 % $F4/80^+$ cells in the harvested cell populations using FITC-conjugated anti-mouse F4/80 monoclonal antibodies (mAb, BM8) (data not shown). BMDCs were differentiated from freshly isolated murine bone marrow cells in complete RPMI 1640 containing 20 ng/mL recombinant murine granulocyte–macrophage colony-stimulating factor (Peprotech) and 10 ng/mL recombinant murine IL-4 (Peprotech) for 7 days. $CD11c^+$ cells were further enriched using FACSAria cell sorter (Becton–Dickinson) after staining with FITC-conjugated anti-mouse CD11c (N418, BioLegend) cell marker (cell purity ≥98 %). Highly purified naïve T cells were prepared from the inguinal lymph nodes of WT mice. In brief, single-cell suspensions were prepared by gentle teasing of inguinal lymph node tissues in complete RPMI 1640 medium. Naïve T cells were sorted after staining with the following mAbs (BioLegend): FITC-conjugated anti-mouse/human CD44 (IM7), phycoerythrin (PE)-conjugated anti-mouse CD62L (MEL-14), Percp/Cy5.5 anti-mouse CD4 (RM4-4), and allophycocyanin-conjugated anti-mouse CD25 (3C7). The post-sorting purity of $CD4^+CD25^-CD44^{low}CD62L^{high}$ T cells was ≥98 %.

Conidial Phagocytosis in BMDMs

In brief, FITC-labeled conidia suspensions were incubated in 2×10^6/mL of BMDMs at 37 °C. At two different time points (30 and 120 min), the cells were pelleted and resuspended in 300 μL phosphate-buffered saline (PBS). Phagocytosis of FITC-labeled conidia by BMDMs was determined on a BD FACSCalibur system.

Intracellular ROS Production in BMDMs

For evaluation of ROS production, a total of 5×10^3 BMDMs were added to each well of 96-well microplates and incubated with serum-free DMEM containing 1 mM of 2′,7′-dichlorodihydrofluorescein diacetate (CAS No: 2044-85-1, Sigma-Aldrich) for 20 min at 37 °C. Cells were gently washed three times, and cultured in serum-free DMEM containing zymosan (100 μg/mL, CAS No: 58856-93-2, Sigma-Aldrich) and *P. verrucosa* conidia (multiplicity of infection [MOI] 10) for another 120 min at 37 °C. BMDMs were washed twice with PBS, and fluorescence was measured spectrophotometrically at excitation and emission wavelengths of 485 nm and 540 nm, respectively.

Conidia Killing in BMDMs

Briefly, 2×10^6 cells/mL of BMDMs were mixed with live *P. verrucosa* conidia (MOI 10) and incubated

at 37 °C for 30 min. After washing with PBS three times, the cells were resuspended with 0.5 mL culture medium and incubated for another 30 or 120 min. At the indicated time points, 0.5 mL of 1 ‰ Triton X-100 was added to lyse the BMDMs. Finally, 100 μL of the samples was plated on Sabouraud's agar (Becton–Dickinson Biosciences, San Diego, CA, USA) with a series of diluted solutions. After 7 days of incubation, the numbers of CFU were counted, and the killing percentage was determined by the formula: percent killing = [1 − (CFU at 30 or 120 min/CFU at 0 min)] × 100 %.

Phenotypic Analysis in BMDCs

BMDCs were suspended to a concentration of 1×10^6 cells/mL and exposed to heat-killed *P. verrucosa* (HKPV) conidia (DC:conidia = 1:10) at 37 °C. After 24 h of infection, stimulated BMDCs were harvested to assess the phenotypic changes by labeling with the following mAbs (BioLegend): PE-conjugated anti-mouse CD80 (16-10A1), CD86 (GL-1), and I-A/I-E (M5/114.15.2). The labeled cells were acquired on a BD FACSCalibur system and analyzed with Flowjo7.6 software.

In Vitro T Cell Differentiation Assay

Purified WT and *Card9* KO BMDCs were incubated with HKPV conidia (DC:conidia = 1:10) for 24 h at 37 °C. For in vitro T cell differentiation assay, BMDCs receiving different stimuli as described above were incubated with purified naïve T cells (DC:T = 1:10) for another 7 days at 37 °C. Living cells were restimulated with Cell Stimulation Cocktail (Cat No: 00-4975, eBioscience) for 6 h at 37 °C to promote intracellular accumulation of secreted proteins. Intracellular cytokine staining was performed with the following mAbs (Biolegend): FITC-conjugated anti-mouse CD4 (RM4-4) and allophycocyanin-conjugated anti-mouse IL-17A (TC11-18H10.1). Samples were acquired on a BD FACSCalibur system and analyzed with Flowjo7.6 software.

In Vitro, Ex Vivo and In Vivo Supernatants for Cytokine Protein Determination

In vitro cell culture supernatants from stimulated BMDMs or BMDCs were generated using BMDMs or BMDCs infected with live *P. verrucosa* conidia or HKPV (MOI 10). Supernatants were collected from in vitro cultures after 24 h of incubation at 37 °C and 5 % CO_2. In vitro cell culture supernatants from in vitro T cell differentiation assay described above were collected from in vitro cocultures after 7 days of incubation at 37 °C and 5 % CO_2. Ex vivo cell culture supernatants were generated using single-cell suspension from the popliteal and inguinal draining lymph nodes harvested from mice 7 days after infection. After stimulated with live HKPV (MOI 10), supernatants were collected from ex vivo cocultures after 5 days of incubation at 37 °C and 5 % CO_2. In vivo footpad homogenates from infected mice were obtained from tissue homogenates of *P. verrucosa* - injected footpads 7 days after infection. In vitro, ex vivo and in vivo supernatants for cytokine protein determination were measured using cytometric bead array technology (Becton–Dickinson) according to the manufacturer's instructions.

Statistical Analysis

Data are expressed as mean ± SD. Graphs were plotted using Graph Pad Prism 5 software. Survival curves were compared by a log-rank (Mantel Cox) test. Differences between groups were examined for statistical significance using SPSS 16.0. The results were analyzed using an independent analysis of variance test. $P < 0.05$ was considered statistically significant, and $P < 0.01$ was considered highly significant. Unless otherwise specified, all studies for which data are presented are representative of at least two independent experiments.

Results

Increased Susceptibility of *Card9* KO Mice to Subcutaneous *P. verrucosa* Infection

Utilizing this murine model of subcutaneous *P. verrucosa* infection, we observed natural resistance of WT and *Card9* KO mice inoculated subcutaneously with *P. verrucosa.* Infected WT mice developed small lesions that resolved spontaneously via self-healing by 8 weeks after infection (Fig. 1a). By contrast, infected *Card9* KO mice were prone to chronic infections and developed rapidly growing, large, nonhealing lesions.

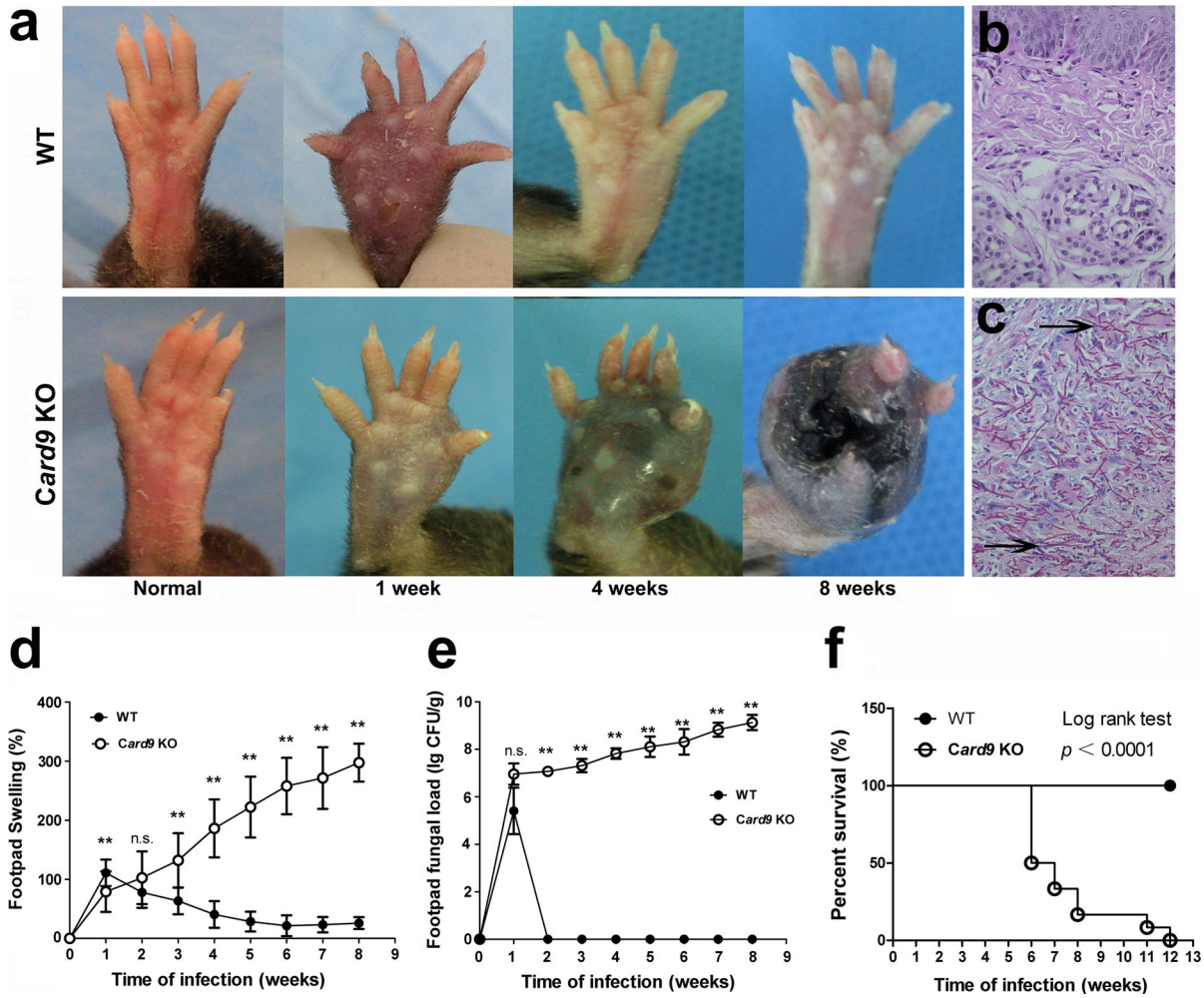

Fig. 1 CARD9 deficiency leads to increased susceptibility to *P. verrucosa*-induced subcutaneous infections. WT and *Card9* KO mice were, respectively, inoculated subcutaneously with 1×10^7 CFU of live *P. verrucosa* conidia. **a** Natural course of *P. verrucosa* infection in WT ($n = 6$) and *Card9* KO mice ($n = 6$). Representative images of normal footpads (before inoculation) and infected footpads (1, 4, and 8 weeks post-inoculation). **b**, **c** A normal skin tissue structure was observed in WT mice, while pigmented fungal hyphae, pseudohyphae, conidia, and spores positive for PAS staining were observed in *Card9* KO mice at 8 weeks post-infection. Representative images from WT (**b**) and *Card9* KO (**c**) mice are shown at magnifications of ×400 (The fungal forms are indicated by *arrows*). **d** Footpad swelling of *P. verrucosa*-infected WT ($n = 6$) and *Card9* KO mice ($n = 6$) at different time points after infection. Data are shown as the mean ± SD of six samples per group. **e** Footpad fungal burden of *P. verrucosa*-infected WT ($n = 6$) and *Card9* KO mice ($n = 6$) at different time points after infection. Data are shown as the mean ± SD of six samples per group. **f** Survival analysis of WT and *Card9* KO mice after *P. verrucosa* infection. Survival of WT ($n = 12$) and *Card9* KO mice ($n = 12$) was monitored for 3 months following subcutaneous infection with 1×10^7 CFU of live *P. verrucosa* conidia. Survival data were analyzed with the log-rank test. $^{**}P < 0.01$

At 8 weeks post-infection, the infected footpads of *Card9* KO mice presented swelling, abscess, ulceration, and crust. In addition, transepithelial liberation of the abscess and acral mutilation in the infected footpad were observed (Fig. 1a). Histological examination of the infected footpads revealed different patterns by 8 weeks after infection. Histological sections in WT mice showed a normal skin tissue structure (Fig. 1b), whereas pigmented fungal hyphae, pseudohyphae, conidia, and spores positive for PAS staining were observed in the infected footpads of *Card9* KO mice (Fig. 1c). These results showed that the in vivo phenotype of the *P. verrucosa* subcutaneous infection of *Card9* KO mice could mimic the clinical and

histological characteristics of subcutaneous phaeohyphomycosis.

Footpad swelling, which can reflect the inflammatory response of edema and infiltrate, was monitored weekly as a measure of the severity of local infection (Fig. 1d). In WT mice, footpads showed peak swelling at 1 week post-infection, and then, the swelling gradually decreased. In contrast, the infected footpad volume of *Card9* KO mice continually increased throughout the 8-week observation period. To determine whether greater footpad swelling is correlated with a higher fungal burden, we quantified the fungal loads of *P. verrucosa* in the infected footpads. Footpad fungal burdens were significantly higher in *Card9* KO mice (Fig. 1e). Furthermore, CARD9 was shown to be essential for murine survival following subcutaneous infection with *P. verrucosa* (Fig. 1f): we observed 100 % mortality in the *Card9* KO mice at 12 weeks post-infection and no mortality in the C57BL/6 WT mice.

Disseminated and Systemic Infections in *Card9* KO Mice at the Later Phase of Infection

In order to determine whether the high mortality of infected *Card9* KO mice was directly associated with disseminated and systemic infection, we analyzed the histology of draining lymph nodes and visceral organs from the dead *Card9* KO mice with H&E or PAS staining. The results showed that the pathogens had spread to the brain, lungs, liver, spleen, kidney, and draining lymph nodes of *Card9* KO mice at the late phase of infection (Fig. 2). The fungal forms are not observed in the histology samples of draining lymph nodes and visceral organs from wild-type mice (data not shown).

Th17 Response is Responsible for Protective Adaptive Immunity Against *P. verrucosa*

Given that the footpad swelling and fungal burdens in WT and *Card9* KO mice began to diverge at 1 week post-infection (Fig. 1d, e), we speculated that CARD9 may promote the elimination of the pathogens by affecting the immune response at a local focus of infection at the early phase. Despite similar fungal burdens between the groups at this time point (Fig. 1e), TNF-α, IL-1β, IL-6, and IL-17A levels were markedly reduced in the *Card9* KO mice compared to the WT mice at 1 week post-infection (Fig. 3), indicating a decreased Th17-specific response in *Card9* KO mice at the early stage of infection.

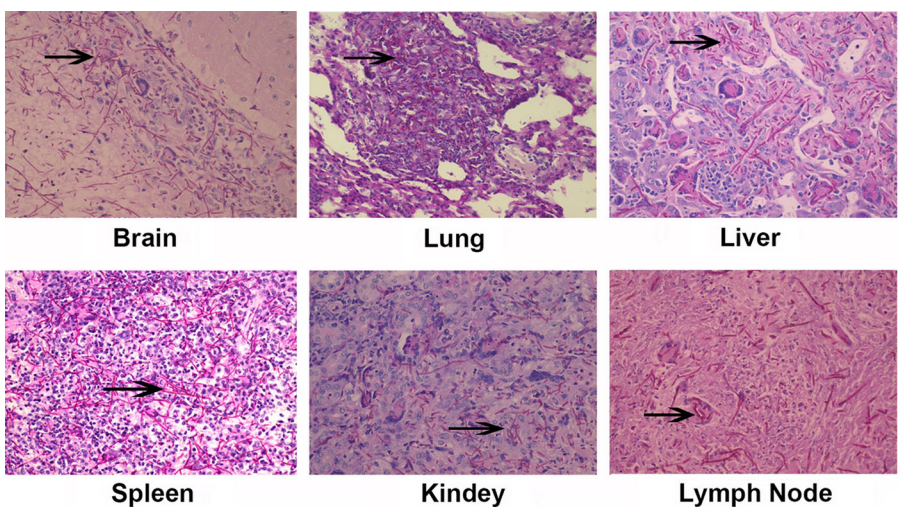

Fig. 2 Disseminated and systemic infection of *P. verrucosa* in *Card9* KO mice. Tissue sections from dead *Card9* KO mice were stained with PAS, and pigmented fungal hyphae, pseudohyphae, conidia, and spores positive for PAS staining were observed. Representative histological images of the brain, lung, liver, spleen, kidney, and lymph node from *Card9* KO mice are shown at magnifications of ×400 (The fungal forms are indicated by *arrows*)

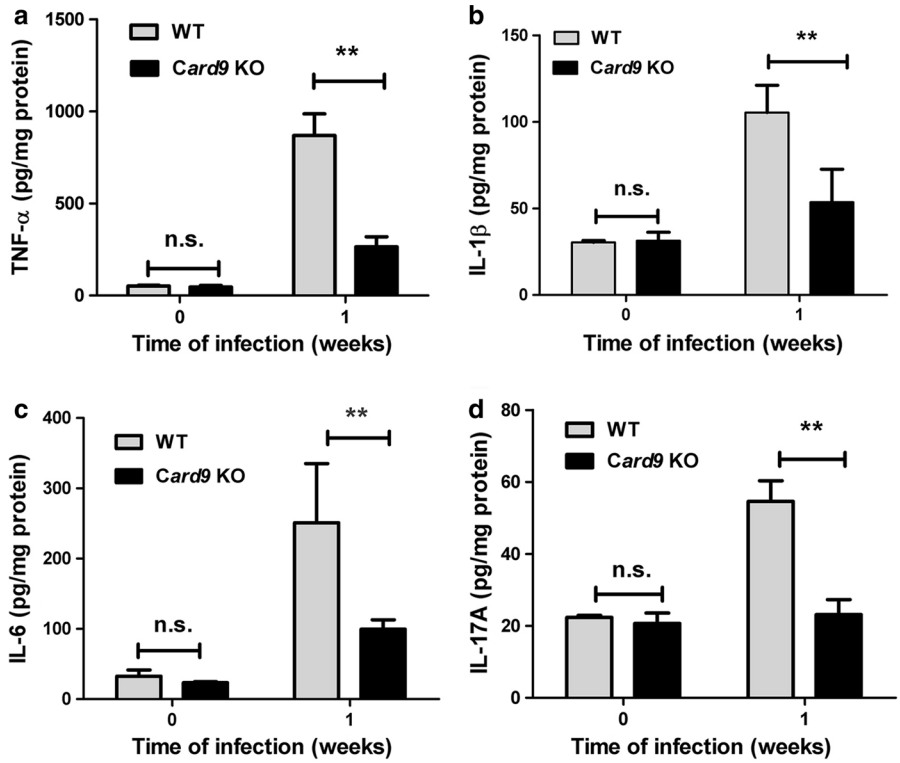

Fig. 3 *Card9* KO mice failed to mount efficient Th17 responses against *P. verrucosa* infection. **a–d** Cytokine levels in footpad homogenates from infected WT ($n = 6$) and *Card9* KO ($n = 6$) mice were determined using the BD cytometric bead assay at 1 week post-infection. Data shown are for TNF-α (**a**), IL-1β (**b**), IL-6 (**c**), and IL-17A (**d**). Week 0 represents data from uninfected mice. Data are shown as the mean ± SD of six samples per group. $^{**}P < 0.01$; *n.s.* not significant

Defective Responses to *P. verrucosa* Infection in *Card9* KO BMDMs

In response to invading pathogens, macrophages engage in phagocytosis and rapidly ROS generation, serving as the initial step of microorganism killing [21]. Given that the *Card9* KO mice were defective in clearing *P. verrucosa* infection, we further investigated the role of CARD9 in the killing of *P. verrucosa* in macrophages. To determine whether CARD9 controls the phagocytosis activity of BMDMs, conidial uptake was measured and was found to be similar in infected BMDMs from WT and *Card9* KO mice at 30 or 120 min post-infection (Fig. S1a, additional data are given in Online Resource 1). Furthermore, we investigated ROS generation in BMDMs after stimulation. The results demonstrated that *P. verrucosa* increased ROS production to similar levels in both WT and *Card9* KO BMDMs (Fig. S1b, additional data are given in Online Resource 1). *Card9* KO BMDMs exhibited severe defects in the production of TNF-α (Fig. 4a) and IL-6 (Fig. 4b) compared with WT cells. Finally, we found that *Card9* KO BMDMs exhibited significantly impaired fungicidal activity against *P. verrucosa* compared with WT cells at 30 and 120 min (Fig. 4c).

Defective Responses Against *P. verrucosa* in *Card9* KO BMDCs

DC activation is defined by high levels of major histocompatibility complex (MHC) II, the costimulatory molecules CD80 and CD86, and cytokines secretion, which enable the cells to present antigens to T cells and promotes T cell differentiation and expansion [22, 23]. Incubation with HKPV conidia for 24 h resulted in increased expression of CD80, CD86, and MHC II on BMDCs (Fig. S2, additional data are given in Online Resource 1); however, there was no significant difference between the two groups before and after stimulation. Therefore, BMDCs undergo normal phenotypic activation upon exposure to HKPV conidia. As shown in Fig. 4d–f, incubation with HKPV conidia resulted in impaired secretion of IL-1β, IL-6, and IL-23p19/p40 from *Card9* KO BMDCs.

Th17 Cell Differentiation Requires Card9

Because *Card9* KO mice failed to recruit IL-17A in the infected footpad (Fig. 3d), we further investigated whether Card9 governs the differentiation of effector T cells during the *P. verrucosa*-priming phase. Three

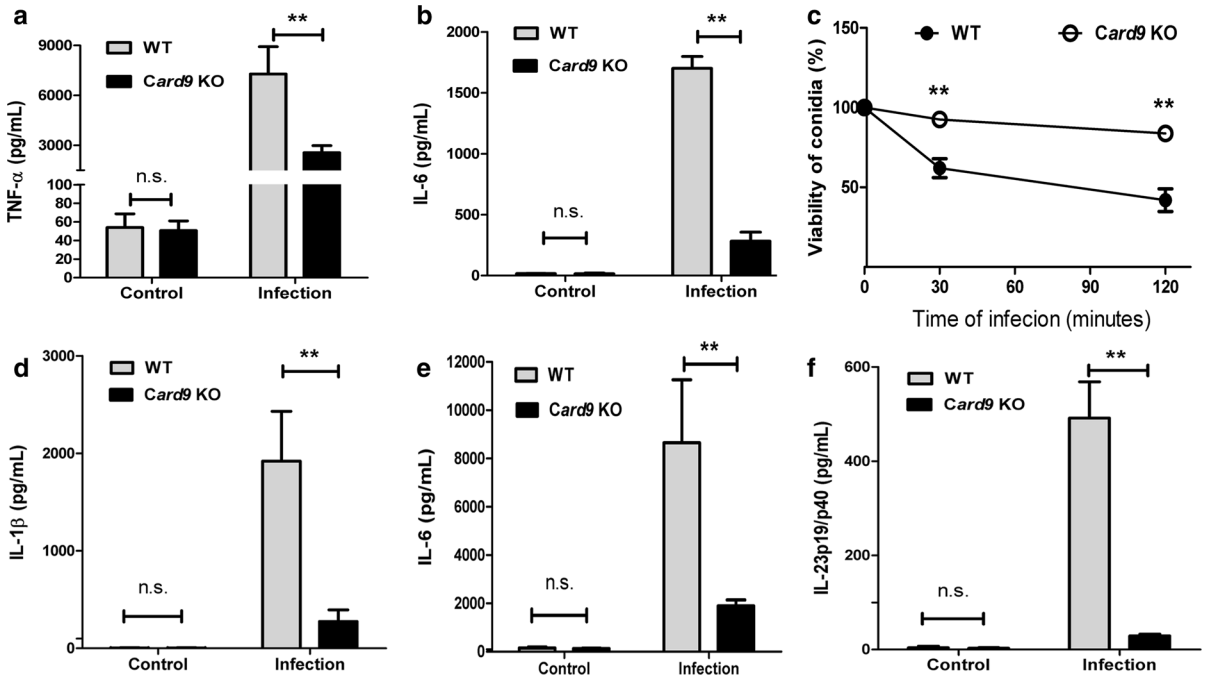

Fig. 4 Defective responses to *P. verrucosa* infection in *Card9* KO BMDMs and BMDCs. **a**, **b** Cytokine production by BMDMs after exposure to *P. verrucosa* conidia. WT and *Card9* KO BMDMs were incubated with *P. verrucosa* for 24 h at 37 °C. TNF-α and IL-6 production in culture supernatants were assessed using the BD cytometric bead assay. Data are shown as the mean ± SD of six samples per group. **c** Killing of *P. verrucosa* conidia by WT and *Card9* KO BMDMs. WT and *Card9* KO BMDMs were incubated with *P. verrucosa* for 30 or 120 min at 37 °C. The killing efficacy of BMDMs against *P. verrucosa* conidia was assessed by a serial dilutions assay. Data are expressed as the percentage of CFU at 30 or 120 min with respect to that at 0 min. Data are shown as the mean ± SD of six samples per group. **d**–**f** Impaired cytokines secretion of stimulated BMDCs. BMDCs were stimulated with HKPV at a DC:conidia ratio of 1:10 for 24 h at 37 °C. After stimulation, the supernatant was collected and IL-1β (**d**), IL-6 (**e**), and IL-23p19/p40 (**f**) production was detected using the BD cytometric bead assay. Data are shown as the mean ± SD of six samples per group. $^{**}P < 0.01$; *n.s.* not significant

independent approaches were performed to analyze T cell differentiation. First, we harvested activated T cells at the peak of expansion from the draining lymph nodes and stimulated them ex vivo with HKPV. T cells from WT mice produced more IL-17A protein in response to fungal than did *Card9* KO T cells (Fig. 5a). In a second approach, we cocultured allogeneic WT naïve T cells with BMDCs stimulated with HKPV conidia. T cells cocultured with *Card9* KO BMDCs produced less IL-17A than did cocultures with wild-type BMDCs in cell culture supernatants (Fig. 5a). Third, coculture of allogeneic naïve T cells with WT BMDCs stimulated with HKPV conidia elicited a robust frequency of IL-17A-producing Th17 cells, whereas this frequency was significantly lower in *Card9* KO BMDC/T cell cultures after stimulation (Fig. 5b–d), indicating the impaired Th17-polarizing abilities of *Card9* KO BMDCs. Thus, Card9 signaling is requisite for the differentiation of Th17 cells during the priming phase of *P. verrucosa*-induced immunity.

Discussion

Owing to its nonspecific clinical findings and chronic course, it has thus far been difficult to observe the natural infection history of phaeohyphomycosis. Here, we utilized intraplantar injection with *P. verrucosa* in WT and *Card9* KO mice to establish a murine model of subcutaneous phaeohyphomycosis. Infected WT mice eventually developed the ability of self-healing, whereas infected *Card9* KO mice displayed clinical and histological characteristics similar to phaeohyphomycosis, suggesting that *Card9* KO mice may serve as a useful animal model for studying the protective immune response of phaeohyphomycosis.

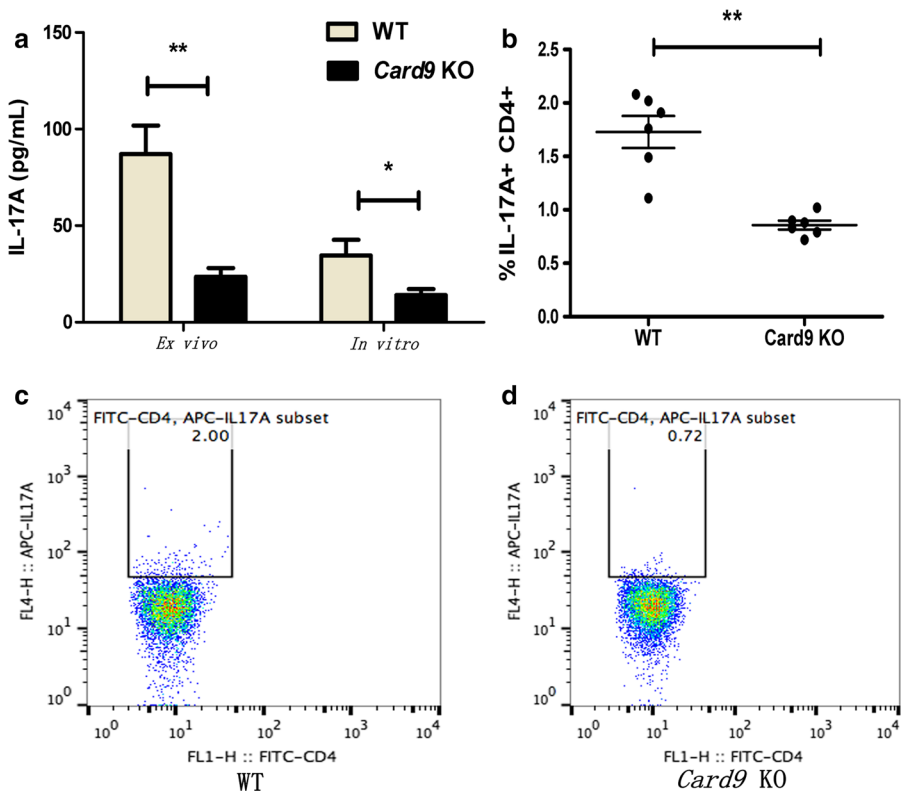

Fig. 5 Card9 signaling is required for the development of Th17 cells in responses to *P. verrucosa* infection. **a** IL-17A production in ex vivo and In vitro cell culture supernatants. Ex vivo coculture was performed with primed T cells from draining lymph nodes of wild-type and *Card9* KO mice, which were cocultured ex vivo with HKPV for 5 days. For in vitro coculture, BMDCs from wild-type and *Card9* KO mice were cocultured with HKPV for 24 h, and then were incubated with Naïve T cells for another 7 days. IL-17A production from ex vivo and in vitro coculture supernatant was measured by CBA. Data are shown as the mean ± SD of six samples per group. **b–d** Proportions of IL-17A-producing Th17 cells ($CD4^+$/$IL\text{-}17A^+$) in primed T cells. Stimulated WT and *Card9* KO BMDCs were cocultured with WT naïve T cells at a DC:T cell ratio of 1:10 for 7 days at 37 °C. After coculture, the frequencies of the primed T cells that produced IL-17A were compared between WT and *Card9* KO mice (**b**). Individual samples are shown as the dots and the mean ± SD of six samples per group are shown as the *lines* in scatter dot plot. Representative flow cytometric dot plots of IL-17A-producing Th17 cells in WT (**c**) and *Card9* KO (**d**) mice. $^*P < 0.05$; $^{**}P < 0.01$; *n.s.* not significant

Furthermore, *Card9* KO mice showed markedly lower survival, significantly stronger footpad swelling, and greater fungal loads in the footpads, which demonstrated that this model is more susceptible to *P. verrucosa* infection. Taken together, we provided compelling evidence for a critical role of CARD9 in controlling *P. verrucosa* clearing and in the development of protective immunity against subcutaneous *P. verrucosa* infections in this mouse model.

In this study, we observed that infected *Card9* KO mice began to die as of 6 weeks post-infection. Furthermore, histological findings of draining lymph nodes and visceral organs from the dead *Card9* KO mice with H&E or PAS staining showed that the pathogens spread to the local draining lymph nodes, lungs, liver, spleen, and kidney, as well as the central nervous system, at the late phase of infection. In view of the involvement of multiple visceral organs and the multiple independent lesions in the infected organs, the hematogenous spread of *P. verrucosa* is a likely mechanism of infection. In general, localized cutaneous and subcutaneous nodules are a common manifestation of phaeohyphomycosis, but immunocompromised patients are at increased risk of subsequent dissemination [1]. Several authors have speculated that systemic phaeohyphomycosis may hematogenously disseminate to multiple organs and ultimately reach the brain and bones [24, 25].

Therefore, based on the results of our animal model and previous clinical reports, regular follow-up should be performed to closely monitor the occurrence of systemic and disseminated infection in phaeohyphomycosis patients, especially in immunocompromised individuals.

The innate immune system constitutes the first line of host defense against pathogens, which is mediated mainly by phagocytic cells, APCs, and neutrophils. CARD9 is expressed primarily in myeloid cells, especially in neutrophils, macrophages, and DCs. Therefore, CARD9 deficiency may contribute to susceptibility through the effects on these cells. Our previous study demonstrated that CARD9-deficient polymorphonuclear neutrophils exhibited defects in *P. verrucosa* killing and the production of pro-inflammatory cytokines [26]. Therefore, in the present study, we sought to further investigate the effect of CARD9 deficiency on macrophages and DCs upon *P. verrucosa* infection.

The classic polarization and activation of macrophages into potent pro-inflammatory cells are generally characterized by the generation of reactive oxygen and nitrogen species and pro-inflammatory cytokines, including TNF-α and IL-6 [27, 28]. Previous studies demonstrated that impaired TNF-α and IL-6 production resulted in insufficient recruitment and activation of myeloid cells (e.g., neutrophils and macrophages) at the sites of infection [29, 30]. The present study demonstrated that *Card9* KO BMDMs had a completely normal capacity of phagocytosis and ROS generation, suggesting that CARD9 does not play a role in the normal recognition and signaling for these immediate responses in BMDMs, which is consistent with several previous studies [12, 31]. Furthermore, *Card9* KO BMDMs were unable to release sufficient TNF-α and IL-6 in response to *P. verrucosa* challenge. So, we speculated that Card9 may mediate host resistance to infection with *P. verrucosa* through the recruitment and activation of neutrophils and/or phagocytes. Finally, *Card9* KO BMDMs presented impaired killing activity compared with WT BMDMs when exposed to *P. verrucosa*, which might explain why the pathogens were not readily eliminated in infected *Card9* KO mice. Collectively, our findings demonstrate that CARD9 deficiency underlies the compromised host resistance to *P. verrucosa* in macrophages, and that the impaired responsiveness to *P. verrucosa* infection in *Card9* KO BMDMs is mainly a consequence of defects in conidia killing and pro-inflammatory cytokine production, and not ROS generation and phagocytotic ability. Moreover, although *Card9* KO BMDCs undergo normal phenotypic activation upon exposure to HKPV conidia, we found that the lack of Card9 in BMDCs suppressed IL-1β, IL-6, and IL-23p19/p40 production, which favors Th17 T cell expansion, activation, and differentiation. Thus, Card9 governs the expression of these cytokines that are instrumental in driving differentiation of Th17 cells and likely affects the differentiation phenotype of T cells in *Card9* KO mice. Collectively, these results suggested that CARD9 deficiency attenuates the innate immune response to *P. verrucosa* challenge, which can explain in part the impaired ability of *P. verrucosa* clearing in infected *Card9* KO mice.

Despite the crucial roles of Th1 cells in the protective immunity against fungal infection [32, 33], the role of Th17 cells is less consistent [14, 34–36]. These previous studies suggest that impaired Th17 cell development seems not to be a general feature of CARD9 deficiency in invasive fungal infections. Therefore, we hope to identify the specific CARD9 signaling pathways that might drive the development of Th17 cells after exposure to *P. verrucosa* infection. In vivo, infected *Card9* KO mice showed markedly decreased TNF-α, IL-1β, IL-6, and IL-17A production in footpad homogenates compared with WT mice. These results suggested that reduced Th17 cell immune response in the early immunity phase might be a reason for the compromised host susceptibility to *P. verrucosa* infection. The expression of IL-17A in In vitro and ex vivo cell culture supernatants was significantly lower in *Card9* KO group compared with WT group. Furthermore, the in vitro T cell differentiation assay showed that the number and frequency of IL-17-producing Th17 cells were reduced in the *Card9* KO mice compared to the WT group. Collectively, these results suggested that Card9 signaling is required for the development of Th17 cells in responses to *P. verrucosa* infection. A similar observation has been reported by Wang, H et al., who demonstrated that the adaptor Card9 is essential for the acquisition of vaccine-induced immunity and the development of vaccine-induced Th17 cells against three systemic dimorphic fungi of North America (*Blastomyces dermatitidis*, *Histoplasma capsulatum*, and *Coccidioides posadasii*) in the setting of fungal vaccine models [37]. However, the limitations

of our study is that it cannot be excluded that innate IL-17-producing cell subsets participate in the IL-17 response in the foot of infected mice, such as TCR-γδ T cells, innate lymphoid cells (ILC3), NK and NKT cells from the ex vivo and in vitro experimental data. So, further studies are required to make sure whether Card9 has an impact on these alternate sources of IL-17.

Taken together, our findings indicate an indispensable role of CARD9 in regulating the innate immune and Th17-mediated adaptive immune responses against dematiaceous fungal infections. Future studies are needed to further identify the entire pathway that mediates the host-pathogen interactions and investigate the method to restore the immune response in patients, which may facilitate personalized immunotherapy in the near future.

Acknowledgments We thank Dr. Xin Lin for kindly providing the *Card9* knockout mice; we thank Zhe Wan at the Department of Dermatology, Peking University First Hospital, for isolation and identification of the pathogen; Hao Zhang at the Department of Dermatology, Peking University First Hospital, for assistance with image processing; and Huihui Liu, Department of Hematology, Peking University First Hospital, for technical advice on the in vitro functional analyses of BMDCs. The authors are grateful for the financial support of National Natural Science Foundation of China (Grant 81472890) and Peking University (PKU) 985 Special Funding for Collaborative Research with PKU Hospitals (Grant 2014-1-3).

Compliance with Ethical Standards

Conflict of interest All the co-authors declare that they have no relevant conflicts of interest.

Ethical Approval All procedures performed in studies involving animals were in accordance with institutional guidelines and were approved by the Institutional Ethics Committee of Peking University First Hospital in accordance with the National Institutes of Health Animal Care Guidelines.

References

1. Chowdhary A, Perfect J, de Hoog GS. Black molds and melanized yeasts pathogenic to humans. Cold Spring Harb Perspect Med. 2015;5(8):a019570. doi:10.1101/cshperspect.a019570.
2. Revankar SG, Sutton DA. Melanized fungi in human disease. Clin Microbiol Rev. 2010;23(4):884–928. doi:10.1128/CMR.00019-10.
3. Revankar SG. Dematiaceous fungi. Mycoses. 2007;50(2):91–101. doi:10.1111/j.1439-0507.2006.01331.x.
4. Loures FV, Pina A, Felonato M, Feriotti C, de Araujo EF, Calich VL. MyD88 signaling is required for efficient innate and adaptive immune responses to *Paracoccidioides brasiliensis* infection. Infect Immun. 2011;79(6):2470–80. doi:10.1128/IAI.00375-10.
5. Sousa Mda G, Reid DM, Schweighoffer E, Tybulewicz V, Ruland J, Langhorne J, et al. Restoration of pattern recognition receptor costimulation to treat chromoblastomycosis, a chronic fungal infection of the skin. Cell Host Microbe. 2011;9(5):436–43. doi:10.1016/j.chom.2011.04.005.
6. Romani L. Immunity to fungal infections. Nat Rev Immunol. 2011;11(4):275–88. doi:10.1038/nri2939.
7. Korn T, Bettelli E, Oukka M, Kuchroo VK. IL-17 and Th17 Cells. Annu Rev Immunol. 2009;27:485–517. doi:10.1146/annurev.immunol.021908.132710.
8. Wang X, Wang W, Lin Z, Li T, Yu J, Liu W, et al. CARD9 mutations linked to subcutaneous phaeohyphomycosis and TH17 cell deficiencies. J Allergy Clin Immunol. 2014;133(3):905-8.e3. doi:10.1016/j.jaci.2013.09.033.
9. Roth S, Ruland J. Caspase recruitment domain-containing protein 9 signaling in innate immunity and inflammation. Trends Immunol. 2013;34(6):243–50. doi:10.1016/j.it.2013.02.006.
10. Lionakis MS, Holland SM. CARD9: at the intersection of mucosal and systemic antifungal immunity. Blood. 2013;121(13):2377–8. doi:10.1182/blood-2013-01-480434.
11. Glocker EO, Hennigs A, Nabavi M, Schaffer AA, Woellner C, Salzer U, et al. A homozygous CARD9 mutation in a family with susceptibility to fungal infections. N Engl J Med. 2009;361(18):1727–35. doi:10.1056/NEJMoa0810719.
12. Drewniak A, Gazendam RP, Tool AT, van Houdt M, Jansen MH, van Hamme JL, et al. Invasive fungal infection and impaired neutrophil killing in human CARD9 deficiency. Blood. 2013;121(13):2385–92. doi:10.1182/blood-2012-08-450551.
13. Lanternier F, Pathan S, Vincent QB, Liu L, Cypowyj S, Prando C, et al. Deep dermatophytosis and inherited CARD9 deficiency. N Engl J Med. 2013;369(18):1704–14. doi:10.1056/NEJMoa1208487.
14. Lanternier F, Barbati E, Meinzer U, Liu L, Pedergnana V, Migaud M, et al. Inherited CARD9 deficiency in 2 unrelated patients with invasive Exophiala infection. J Infect Dis. 2015;211(8):1241–50. doi:10.1093/infdis/jiu412.
15. Yan XX, Yu CP, Fu XA, Bao FF, Du DH, Wang C, et al. CARD9 mutation linked to *Corynespora cassiicola* infection in a Chinese patient. Br J Dermatol. 2016;174(1):176–9. doi:10.1111/bjd.14082.
16. Tong Z, Chen SC, Chen L, Dong B, Li R, Hu Z, et al. Generalized subcutaneous phaeohyphomycosis caused by *Phialophora verrucosa*: report of a case and review of literature. Mycopathologia. 2013;175(3–4):301–6. doi:10.1007/s11046-013-9626-3.
17. Gao LJ, Yu J, Wang DL, Li RY. Recalcitrant primary subcutaneous phaeohyphomycosis due to *Phialophora verrucosa*. Mycopathologia. 2013;175(1–2):165–70. doi:10.1007/s11046-012-9602-3.
18. Watanabe K, Kagaya K, Yamada T, Fukazawa Y. Mechanism for candidacidal activity in macrophages activated by recombinant gamma interferon. Infect Immun. 1991;59(2):521–8.
19. Gorjestani S, Yu M, Tang B, Zhang D, Wang D, Lin X. Phospholipase Cgamma2 (PLCgamma2) is key component in Dectin-2 signaling pathway, mediating anti-fungal innate

immune responses. J Biol Chem. 2011;286(51):43651–9. doi:10.1074/jbc.M111.307389.
20. Verdan FF, Faleiros JC, Ferreira LS, Monnazzi LG, Maia DC, Tansine A, et al. Dendritic cell are able to differentially recognize *Sporothrix schenckii* antigens and promote Th1/Th17 response in vitro. Immunobiology. 2012;217(8):788–94. doi:10.1016/j.imbio.2012.04.006.
21. Wu W, Hsu YM, Bi L, Songyang Z, Lin X. CARD9 facilitates microbe-elicited production of reactive oxygen species by regulating the LyGDI-Rac1 complex. Nat Immunol. 2009;10(11):1208–14. doi:10.1038/ni.1788.
22. Mellman I. Dendritic cells: master regulators of the immune response. Cancer Immunol Res. 2013;1(3):145–9. doi:10.1158/2326-6066.CIR-13-0102.
23. Joffre O, Nolte MA, Sporri R, Reis e Sousa C. Inflammatory signals in dendritic cell activation and the induction of adaptive immunity. Immunol Rev. 2009;227(1):234–47. doi:10.1111/j.1600-065X.2008.00718.x.
24. Li DM, Li RY, de Hoog GS, Sudhadham M, Wang DL. Fatal Exophiala infections in China, with a report of seven cases. Mycoses. 2011;54(4):e136–42. doi:10.1111/j.1439-0507.2010.01859.x.
25. Ochiai H, Kawano H, Minato S, Yoneyama T, Shimao Y. Cerebral phaeohyphomycosis: case report. Neuropathol Off J Jpn Soc Neuropathol. 2012;32(2):202–6. doi:10.1111/j.1440-1789.2011.01244.x.
26. Liang P, Wang X, Wang R, Wan Z, Han W, Li R. CARD9 deficiencies linked to impaired neutrophil functions against *Phialophora verrucosa*. Mycopathologia. 2015;179(5–6):347–57. doi:10.1007/s11046-015-9877-2.
27. Martinez FO, Sica A, Mantovani A, Locati M. Macrophage activation and polarization. Frontiers Biosci J Virtual Libr. 2008;13:453–61.
28. Murray PJ, Allen JE, Biswas SK, Fisher EA, Gilroy DW, Goerdt S, et al. Macrophage activation and polarization: nomenclature and experimental guidelines. Immunity. 2014;41(1):14–20. doi:10.1016/j.immuni.2014.06.008.
29. Balloy V, Chignard M. The innate immune response to *Aspergillus fumigatus*. Microbes Infect Inst Pasteur. 2009;11(12):919–27. doi:10.1016/j.micinf.2009.07.002.
30. Takano T, Azuma N, Satoh M, Toda A, Hashida Y, Satoh R, et al. Neutrophil survival factors (TNF-alpha, GM-CSF, and G-CSF) produced by macrophages in cats infected with feline infectious peritonitis virus contribute to the pathogenesis of granulomatous lesions. Arch Virol. 2009;154(5):775–81. doi:10.1007/s00705-009-0371-3.
31. Goodridge HS, Shimada T, Wolf AJ, Hsu YM, Becker CA, Lin X, et al. Differential use of CARD9 by dectin-1 in macrophages and dendritic cells. J Immunol. 2009;182(2):1146–54.
32. Xue J, Chen X, Selby D, Hung CY, Yu JJ, Cole GT. A genetically engineered live attenuated vaccine of *Coccidioides posadasii* protects BALB/c mice against coccidioidomycosis. Infect Immun. 2009;77(8):3196–208. doi:10.1128/IAI.00459-09.
33. Chai LY, van de Veerdonk F, Marijnissen RJ, Cheng SC, Khoo AL, Hectors M, et al. Anti-Aspergillus human host defence relies on type 1 T helper (Th1), rather than type 17 T helper (Th17), cellular immunity. Immunology. 2010;130(1):46–54. doi:10.1111/j.1365-2567.2009.03211.x.
34. Chamilos G, Ganguly D, Lande R, Gregorio J, Meller S, Goldman WE, et al. Generation of IL-23 producing dendritic cells (DCs) by airborne fungi regulates fungal pathogenicity via the induction of T(H)-17 responses. PLoS one. 2010;5(9):e12955. doi:10.1371/journal.pone.0012955.
35. Deepe GS Jr, Gibbons RS. Interleukins 17 and 23 influence the host response to *Histoplasma capsulatum*. J Infect Dis. 2009;200(1):142–51. doi:10.1086/599333.
36. Whibley N, Jaycox JR, Reid D, Garg AV, Taylor JA, Clancy CJ, et al. Delinking CARD9 and IL-17: CARD9 protects against *Candida tropicalis* infection through a TNF-alpha-dependent, IL-17-independent mechanism. J Immunol. 2015;195(8):3781–92. doi:10.4049/jimmunol.1500870.
37. Wang H, LeBert V, Hung CY, Galles K, Saijo S, Lin X, et al. C-type lectin receptors differentially induce th17 cells and vaccine immunity to the endemic mycosis of North America. J Immunol. 2014;192(3):1107–19. doi:10.4049/jimmunol.1302314.